

RESEARCH ARTICLE

Complex drivers of geomorphic response and habitat formation revealed in multiyear monitoring of Cosumnes River experimental floodplain reconnection

Britne Clifton^{1*}, Joshua H. Viers^{1,2}

1 Environmental Systems, University of California Merced, Merced, California, United States of America,
2 School of Engineering, University of California Merced, Merced, California, United States of America

* bclifton2@ucmerced.edu



OPEN ACCESS

Citation: Clifton B, Viers JH (2024) Complex drivers of geomorphic response and habitat formation revealed in multiyear monitoring of Cosumnes River experimental floodplain reconnection. PLOS Water 3(4): e0000132. <https://doi.org/10.1371/journal.pwat.0000132>

Editor: João Miguel Dias, Universidade de Aveiro, PORTUGAL

Received: March 11, 2023

Accepted: February 8, 2024

Published: April 17, 2024

Copyright: © 2024 Clifton, Viers. This is an open access article distributed under the terms of the [Creative Commons Attribution License](#), which permits unrestricted use, distribution, and reproduction in any medium, provided the original author and source are credited.

Data Availability Statement: Data is accessible via this Dryad repository: <https://doi.org/10.5061/dryad.0p2ngf26q>. All data created during this study is found within the dataset. This data includes all processed and corrected data utilized for the various figures and analysis conducted in this study. Further information is available within the metadata and specific layer/data information provided with the data set.

Funding: This work is supported by Agriculture and Food Research Initiative Competitive Grant no.

Abstract

In this study, we examine a novel levee breach experiment that reconnected a floodplain along the Cosumnes River, California to determine the decadal impact of removing 250 meters of levee and assess the recruitment of large wood. This is the latest study in an ongoing series of investigations 40 years in the making along the largest river on the western slope of the Sierra Nevada without a major dam. We present the findings of this multi-modal investigation here by first measuring the geomorphic alteration of the floodplain surface to quantify the depletion and accretion of sediment across the excavated site. We then identify and quantify the deposition of large wood. Results indicate initiation of anastomosing channel formation and distinct areas of large wood recruitment supporting a naturally evolving lateral levee. Accretion resulted in more than 25,000 m³ of sediment deposition within the original excavation site, the development of multiple sand splays, and natural recruitment of native riparian tree species. We conclude by discussing implications following other approaches to floodplain restoration as a Nature-based Solution. In episodic flow regimes, like in California's Mediterranean-montane hydroclimatic regime, restoring lateral hydrologic connectivity facilitates ecosystem function. Large flood pulse events drive sediment dynamics and geomorphic heterogeneity while enriching biodiversity through biogeochemical fluxes and habitat creation on reconnected floodplains that store floodwaters and reduce peak discharge. These findings support the importance of long-term monitoring efforts of floodplain restoration.

1. Introduction

Within the aquatic terrestrial transition zone, floodplains support some of the most productive and diverse ecosystems on the planet [1–3]. This zone is defined here to include the dynamic channel characteristics [4] and flood pulse events [5] that create geomorphic heterogeneity [6–8] and disturbances, which drive the mosaic of biodiverse riparian forests, floodplains, and

2021-69012-35916 from the USDA National Institute of Food and Agriculture (BC, JHV). The funders had no role in study design, data collection and analysis, decision to publish, or preparation of the manuscript. We thank the Secure Water Future program for their support and Sarah Naumes for invaluable team science coordination.

Competing interests: The authors have declared that no competing interests exist.

other landforms that support complex ecological processes [3, 9–16]. These dynamics include the transitional interface, primarily floodplains, where terrestrial landforms become aquatic habitat [5, 10]. This transitional interface supports the biotic and abiotic processes necessary for diverse habitat structure [17] and elevated ecosystem productivity [14, 18], while also providing a physical canvas for dynamic geomorphic evolution [19, 20].

Once a dynamic interface, anthropogenic land-use activities now conflict with riparian ecosystem functionality [21, 22]. More than 70% of humanity dwells on former floodplains which cover less than 2% of land on earth [2, 23, 24]. Floodplains, though small in area, disproportionately contribute to global hydrogeomorphic cycling. It is estimated that floodplains provide or promote ~25% of all terrestrial ecosystem services [23], including flood mitigation and nutrient cycling [24–26]. Recent studies also suggest, however, that some 90% of the world's floodplains are disconnected and/or developed [2, 22, 24], including up to 98% of floodplains in the United States [27, 28]. Engineered infrastructure, such as levees, are constructed to reduce flood risk. In turn, floodplains are converted for urban and agricultural land uses [28, 29], thereby preventing lateral hydrologic connectivity [2, 30], reducing or eliminating floodplain habitat and dynamic ecosystem feedbacks between geomorphic features and the biophysical responses that drive them [2, 31–33]. Paradoxically, loss of floodplains and biophysical feedbacks reduces floodplain capacity for temporary floodwater storage [24, 25], possibly increasing flood hazards in other locations [25]. By preventing these functions, at least 41 million people in the contiguous United States alone are at risk of serious flooding from pluvial (rainfall) and/or fluvial (riverine) sources, with human populations at risk projected to rise with climate change and expanding development [34].

Restoring active channel-floodplain processes through levee breaches [35–37] or setbacks [38, 39] is a primary means for enhancing ecological functionality. This process-based floodplain restoration approach [40–43] is part of a broader effort to incorporate Nature-based Solutions (NbS) into community resilience planning [44–48]. This so-called “green infrastructure”, and the related “Engineering with Nature” concept [39, 49], are intended to improve climate change resilience and provide protection from extreme flood events [46, 50]. Lateral floodplain re-connectivity with floodwaters has several positive, cascading effects. Reestablishing connectivity facilitates the transfer of nutrient-rich sediment to the floodplain [35, 51] and the creation of heterogeneous landforms [11, 46], in turn supporting elevated biodiversity [45] through niche differentiation [52]. It also has the added benefits of reducing the risk of levee failures and increasing capacity for floodwater storage, reducing flood hazard risk to adjacent or downstream communities [44, 53]. In diminishing human-induced disruptions to the connectivity of riverine and riparian systems [39, 41, 48, 54], NbS can buffer against extreme weather events [55, 56] and simultaneously help mitigate biodiversity loss [1, 46, 57–59].

The conflict between human-engineered land uses and subsequent floodplain disconnection has resulted in loss of ecosystem services over the last several decades [2, 32, 60]. More recent design and implementation of green infrastructure [56, 61], such as the Engineering with Nature [39, 62] approach, has resulted in a more critical evaluation of the potential synergies between flood protection and enhancing NbS [39, 62]. After more than 91% of California's historical riparian landscapes were converted to human uses through river and floodplain development [63], the state is now a focal point for floodplain restoration via reconnection [29, 64, 65]. The Cosumnes River, in particular, has emerged as a test bed for experimental, process-based restoration of NbS through intentional floodplain reconnection [46, 66, 67].

In this paper, we investigate the decadal evolution of a reconnected floodplain along the Cosumnes River, California, and summarize the outcome of a series of investigations that began in the mid-1990s. This floodplain reconnection restoration experiment included four levee breaches with the primary site centered along 250 m of levee excavated to reconnect the

channel to its floodplain. Nichols and Viers (2017) assessed both the pre-treatment floodplain conditions and initial post-connection geomorphological responses as a function of levee breach width. The analysis presented here extends beyond the first-year response to include 6 additional water years and 27 flood pulse events through 2021. In this study, we address the following questions:

1. Since the 2015 study [68], how and where has floodplain topography of the site changed over time, and what is the magnitude of change in surficial sediments?
2. Which geomorphic features have emerged across the study site since its reconnection, and do these observed changes match the expectations set by prior conceptual models?
3. What is the presence and magnitude of large wood accumulation at the study site, and does it contribute to lateral levee development?

We present the findings of this multi-modal investigation by first measuring the geomorphic alteration of the floodplain surface, then evaluating depletion and accretion of sediment, followed by identifying and quantifying the extent of large wood, and concluding with an evaluation of these observations in the context of previous studies and their implications for other similar approaches to floodplain restoration.

2. Material and methods

The Cosumnes River has been the focus of several floodplain reconnection studies [14, 36, 52, 66, 68–70; Fig 1; Table 1] due in large part to its dynamic hydrologic regime. As the only large, unregulated river on the western slope of the Sierra Nevada, the Cosumnes River hydrograph exhibits high dynamism in its magnitude, frequency, and duration of flood pulses [71, 72]. Below we further discuss the dynamics of the Cosumnes River flow regime, various restoration

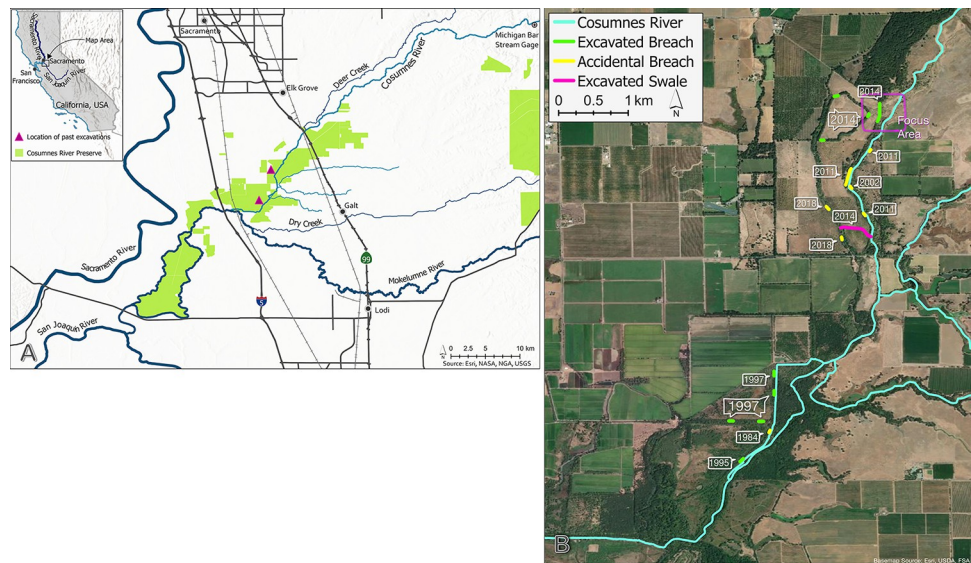


Fig 1. Study site within the Cosumnes River Preserve. A The study site is shown with USGS stream gage 11335000 at Michigan Bar along CRP land management units [73, 74], and B levee breach sites (including a distinction between intentional and accidental breaches) [75]. The Cosumnes River runs from the northeast toward the southwest. The year of each breach is noted. The breaches that were part of planned treatments relevant to this study are identified as “Excavated” and align with breach years in Table 1. The “Focus Area” for this study is also identified. It is primarily the breaches labeled ‘2014’ in the northernmost area of B.

<https://doi.org/10.1371/journal.pwat.0000132.g001>

Table 1. Levee modifications and floodplain reconnection action across the Cosumnes River Preserve.

Date	Outcome & Treatment Details	Publications (Results & Studies)	Area reconnected
1985	Accidental Forest–levee failure prior to CRP acquisition	Eaton, 1998 [93]; Huff & DiGaudio, 2000 [94]; Tu, 2000 [95]; Florsheim & Mount, 2002 [35]; Mount et al., 2002 [52]; Florsheim & Mount, 2003 [51]; Swenson et al., 2003 [36]; Florsheim et al., 2006 [77]; Trowbridge, 2007 [96]; Jeffres et al., 2008 [85]; Swenson et al., 2012 [66]; Hutchinson et al., 2020 [97]	15 acres (6 hectares)
1995	Intentional Forest–levee breach south of Accidental Breach, plot graded & leveled	Eaton, 1998 [93]; Tu, 2000 [95]; Florsheim & Mount, 2002 [35]; Mount et al., 2002 [52]; Florsheim & Mount, 2003 [51]; Swenson et al., 2003 [36]; Ribeiro et al., 2004 [98]; Florsheim et al., 2006 [77]; Trowbridge, 2007 [96]; Jeffres et al., 2008 [85]; Swenson et al., 2012 [66]; Hutchinson et al., 2020 [97]	130 acres (54 hectares)
1997	Corps Breach aka ‘Triangle’– 5.5 miles of levee abandoned, 2 breached levees, plot graded & leveled, a waterfowl pond created within expected flooded area, setback levee construction	Eaton, 1998 [93]; Florsheim & Mount, 2002 [35]; Mount et al., 2002 [52]; Trowbridge, 2002 [70]; Florsheim & Mount, 2003 [51]; Swenson et al., 2003 [36]; Ribeiro et al., 2004 [98]; Ahearn et al., 2006 [88]; Florsheim et al., 2006 [77]; Sheibley et al., 2006 [99]; Jeffres et al., 2008 [85]; Swenson et al., 2012 [66]; Hoagland et al., 2019 [100]; Hutchinson et al., 2020 [97]; Ogaz et al., 2022 [87]	200 acres (81 hectares)
2013	Cougar Wetlands– 2 levee breaches + earthen works to re-establish slough topography, limited planting of individual native species	Beagle et al., 2013 [101]	154 acres (50 hectares)
2014*	Oneto Denier breach– 2 breached levees (1 large + 3 small breaches) + swale	Nichols & Viers, 2017 [68]; Whipple et al., 2017 [71]; D’Elia et al., 2017 [102]; Steger et al., 2019 [89]; Dybala et al., 2019 [26]; Hoagland et al., 2019 [100]	1000 acres (400 hectares)
2017 + TBD	McCormack-Williamson Tract– 3 levee breaches (1 intentional degrading, 2 natural) + future breaches	Hammersmark et al., 2005 [103]; Beagle et al., 2013 [101]	1,489 acres (600 hectares)
TBD	Grizzly Slough	Florsheim et al., 2008 [104]	400 acres (160 hectares)

Table 1: The year, restoration information, resulting publications or studies, and the size of restoration treatments that have included levee breaches or alterations within the Cosumnes River Preserve. The restoration treatment includes any relevant earthen works, planting, or relevant details for the site. *The restoration treatment for the ‘Focus Area’ in [Fig 1B](#).

<https://doi.org/10.1371/journal.pwat.0000132.t001>

activities, geomorphic evolution across a specific floodplain reconnection site, as well as the presence and extent of large wood deposited post reconnection.

2.1. Study site

The predominantly rainfed Cosumnes River drains 2,460 km² of the larger San Joaquin River watershed in central California and is characterized by a Mediterranean-montane climate of cool, wet winters and warm, dry summers [72]. With headwaters at the Sierra Nevada crest (2400 m), and a confluence with the Mokelumne River at sea level, the 80 km Cosumnes River is the largest unregulated river in the Sacramento-San Joaquin Valley.

Cosumnes River discharge is characterized by radical interannual variability with primarily low flows regularly punctuated by peak flows that may be short lived or persist for an extended duration, typically driven by multiple peaks in a given water year (see Whipple et al., (2017) and Booth et al., (2006) for hydrological studies using USGS gage #113350000 at Michigan Bar gage #113350000, identified in [Fig 1A](#)). Since records on the Cosumnes River began in 1907 [76], seasonal flows range from a record high of 2,634 m³s⁻¹ (1997) to a dry stream bed, typically by mid-July. Average winter discharge is 411 m³s⁻¹ while median daily discharge is 46 m³s⁻¹ [71, 76]. Mean annual precipitation throughout the Cosumnes River watershed is approximately 850 mm [68, 72] and is concentrated November–March, primarily in upper elevations [71]. Flood waters connect adjacent floodplains at discharges of 20 to 25 m³s⁻¹ [52, 66],

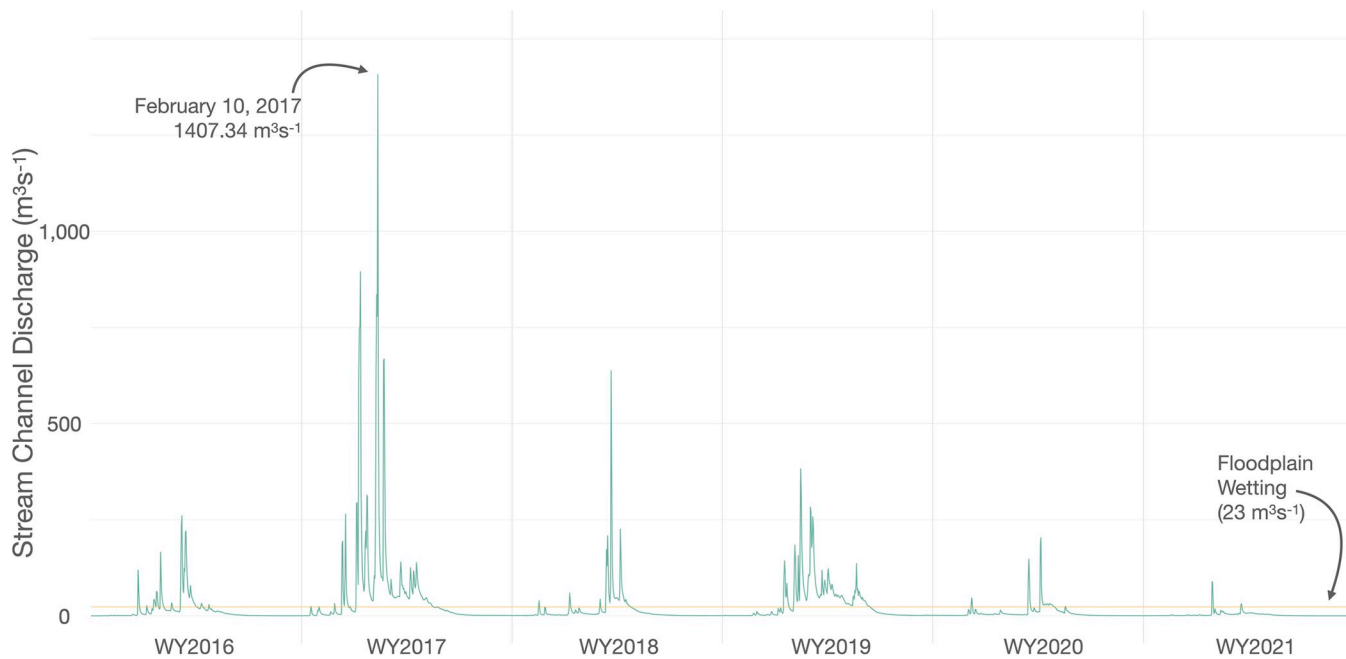


Fig 2. Hydrograph of the USGS stream gage 11335000 at Michigan Bar. The Cosumnes River hydrograph for the USGS stream gage upstream located at Michigan Bar for the duration of the study period (2016–2021). The floodplain wetting stage for the study site is shown as the threshold line at $23 \text{ m}^3 \text{s}^{-1}$ [71].

<https://doi.org/10.1371/journal.pwat.0000132.g002>

[71, 72, 77], and the floodplain wetting stage used in this study follows Whipple et al. (2017), as depicted in Fig 2, of $23 \text{ m}^3 \text{s}^{-1}$ [71]. For this study we consider water years 2016 through 2021, as shown in Fig 2.

Prior to human modification, the Cosumnes River coursed along an anastomosing valley floor [51], characterized by alluvial fans and a geomorphically heterogeneous riparian landscape [78]. Despite the unregulated hydrograph, seasonal river discharge is now impaired by surface water diversions, groundwater withdrawals, land use change, and climatic shifts. Fleckenstein et al., (2004) found that groundwater withdrawal systems for municipal and agricultural demands directly impacted stream flow [79, 80], lowering the local water table and creating regional cones of depression [79]. Concurrently, Young et al., (2009) identified lessening snowmelt runoff as another major influence reducing stream flow [81, 82]. Levee building and channel straightening coincided with widespread land conversion to agricultural uses in the early 20th Century [93], and resulted in floodplain disconnection along much of the lowland river in all but the highest flow events [83]. These findings emphasize the anthropogenic influences that have collectively resulted in the current ephemeral winter wet and summer-dry riverbed experienced in the lowest reaches of the Cosumnes River [72], the variation in river flows are visually documented in Supporting Material.

The unregulated nature of the Cosumnes River, and its frequent winter flood events, has had the paradoxical outcome of limiting urban development and, in so doing, preserving several large riparian forests and adjacent working lands, thus promoting long-term biodiversity conservation [29]. Beginning in 1984 [36], a consortium of land management entities have organized to protect and manage over 20,000 hectares of freshwater, wetland, floodplain, riparian and upland habitats and their associated species [84]. This amalgamation of land parcels, known as the Cosumnes River Preserve (CRP), is protected by a combination of ownership and conservation easements, and has also been the focus of several major restoration efforts, including experimental floodplain reconnection treatments (Table 1). Given these unique

characteristics, CRP has served as an experimental test bed to investigate the multiple ecosystem service benefits of floodplain reconnection, including enhanced biodiversity (e.g., birds, fish) [66, 85–87], carbon sequestration [69, 88, 89], and groundwater recharge [90, 91]. The underlying fundamental drivers of the observed ecosystem service benefits have also been extensively studied, including hydrologic dynamism and geomorphic response [35, 51, 52, 68]. Coupled with restoration treatments implementing horticultural interventions, such as planting with or without irrigation and herbicides [29, 68, 92], decades of observation and monitoring at CRP have provided the basis to quantify differential responses and benefits to hydrogeomorphic connection [35, 36, 68], supplying insight into how floodplain reconnection could benefit other lowland Mediterranean-montane river systems within and beyond California. An overview of floodplain reconnection actions as process-based restoration treatments are provided in [Table 1](#).

Many of the breaches in [Table 1](#) are comparatively narrow (excavated levee sections < 55 m, levee failures < 30 m), whether naturally caused or intentionally excavated. The section of levee removed in 2014 was substantially larger than previous breaches at 250 m wide, allowing for further testing of floodplain reconnection dynamics and expanding previous theoretical frameworks. The Oneto-Denier (OD) levee breach included excavating and leveling a large levee section adjacent to the Cosumnes channel with three additional breaches along an interior “horseshoe” levee as depicted in [Fig 1B](#). These four breaches reconnected nearly 400 hectares of agricultural land (1000 acres) to the river channel [68].

2.2. Measure geomorphic change

In 2014, Nichols and Viers (2017) documented the excavation and leveling followed by the assessment of the first year of reconnection across the ‘OD excavation’ site in 2015. Data collection in both 2014 and 2015 occurred across the full extent of excavated levee and the area of floodplain leveled during the 2014 excavation. To capture GIS and geomorphologic data, they used a Topcon HiperLite + and HiperV real-time kinematic Global Positioning System (rtkGPS) survey equipment alongside a Canon S100 to create a Structure-from Motion DEM. In spring of 2016, and for each subsequent annual survey data collection, a Phoenix LiDAR Alpha AL3-32 deployed on a DJI S1000 octocopter unpiloted aerial vehicle (UAV) and rtkGPS survey equipment were used to capture geomorphic data and measure sediment accretion across the excavation site and reconnected experimental floodplain beyond. LiDAR point cloud based surveys are preferable to rtkGPS surveys because the detail made accessible via the point cloud density possible with LiDAR is impossible to capture by hand [105].

LiDAR point clouds were classified by return interval with LASTools (rapidlasso GmbH, Germany) and filtered for noise and/or error. Points classified as last returns were isolated and used to form the Digital Elevation Models (DEM) for this study. For each year, 0.25 m and 0.5 m DEMs were created to align with the 2014 data format and resolution. Though data collected after 2015 extended beyond the initial excavated levee and leveled area of reconnected floodplain, the DEMs were reduced to the extent of 2014 data coverage for direct comparison. The extent of 2014 data limits the site coverage considered within figures throughout this study.

From 2014 to 2021, the DEM for each year was compared to all previous and subsequent years to create a difference of DEM (DoD) using the approach put forth by Wheaton et al. (2010) applying the Geomorphic Change Detection (GCD) Software, GCD 7, ESRI ArcMap Desktop plugin (ArcMap 10.8.0.12790, Esri, Redlands, California, USA). The GCD tool has two main outputs, raster and tabular data, facilitating comparison between relevant surveys as depicted for 2014 to 2021 in [Fig 3](#) [106]. The extent of [Fig 3](#) demonstrates the limited spatial extent of the 2014 survey.

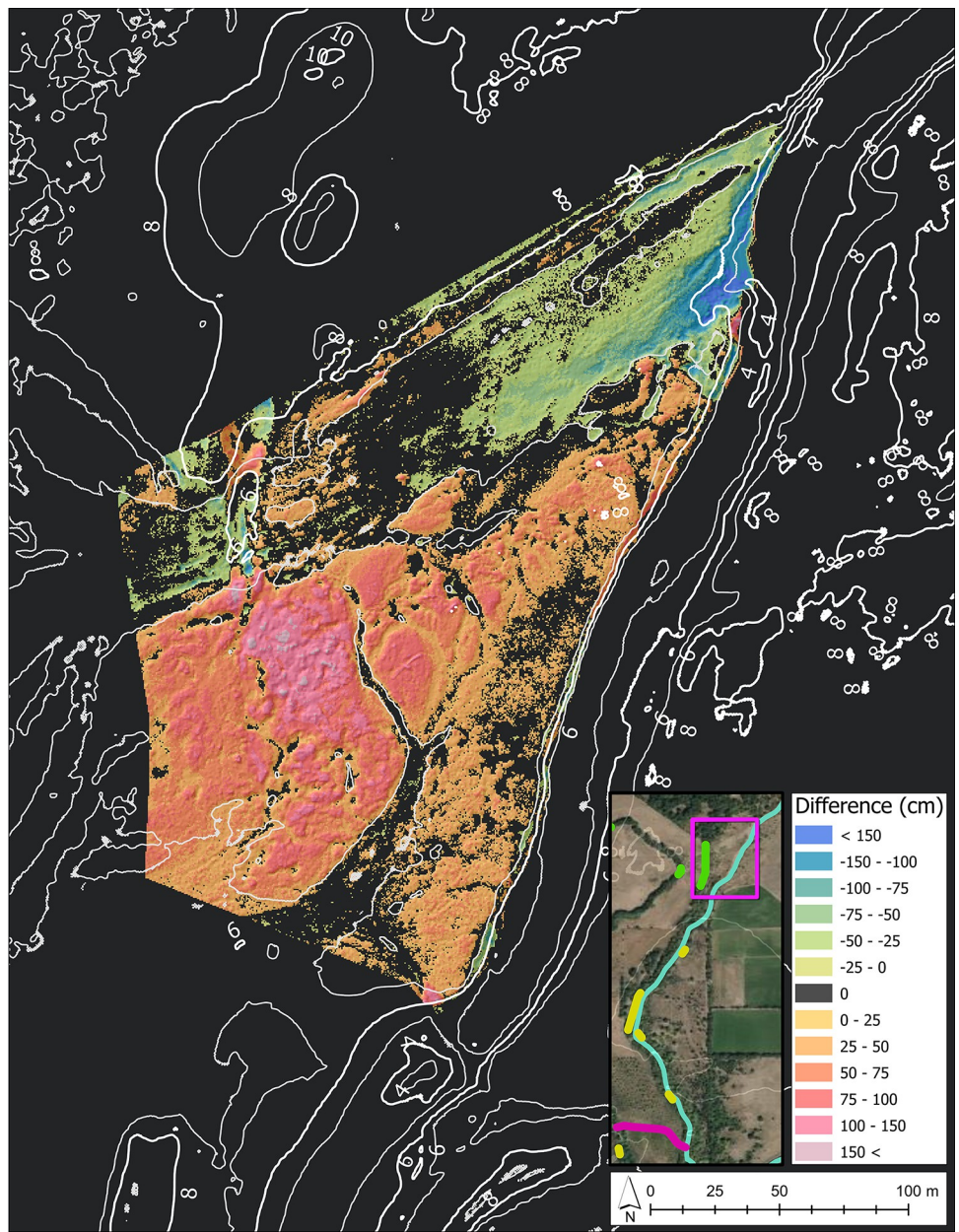


Fig 3. Difference of DEM of 2014 to 2021 within the excavated levee site. The extent of Fig 3 is contextualized within the inset map, a reduced version of Fig 1B. Color represents areas of sediment erosion (blue) to deposition (pink) in centimeters. The background was removed in favor of a uniform black. Elevation is provided by topographic interpretation of the 2021 DEM in meters.

<https://doi.org/10.1371/journal.pwat.0000132.g003>

2.3. Large wood

To evaluate large wood (LWD) deposition and determine the extent of LWD present, a Micasense RedEdge-M multispectral sensor was flown on a FinWing Sabre fixed-wing UAV concurrently with LiDAR data collection discussed in the previous section. The area of interest from the LiDAR survey is mirrored in the multispectral data collection. Raw data were processed, orthorectified, and corrected with Pix4D processing options (Pix4D S.A., Prilly,

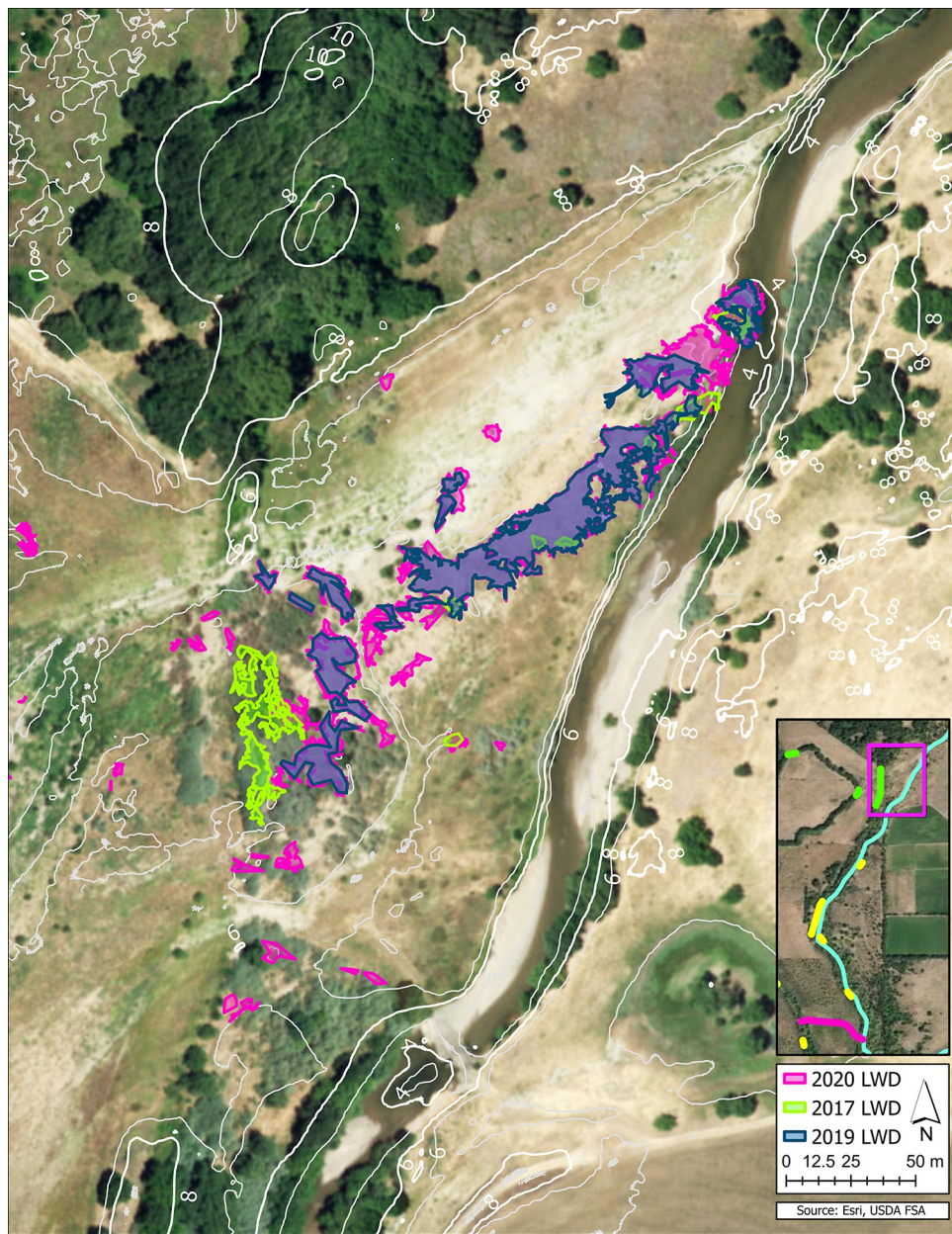


Fig 4. Large wood identified across the reconnected floodplain in 2020. The extent of Fig 4 is matched in Fig 3. The topographic lines may be used to directly compare the two figures and the locations of LWD compared to areas of sediment deposition.

<https://doi.org/10.1371/journal.pwat.0000132.g004>

Switzerland) designed for the RedEdge-M sensor. Concurrent flights for data collections were possible in 2017, 2019, and 2020.

To measure the extent of LWD deposits, spectral bands 1, 3, and 5 (465–485 nm, 663–673, 712–722 nm) were combined to form a false color image that enhanced manual identification and digitization of LWD across the floodplain. The spectral classification allowed for the identification and extraction of large wood features from the surrounding vegetation and sediment in the Digital Surface Model (DSM) as seen in Fig 4. The extent of LWD was confirmed via RTK field survey in 2020. LWD area coverage was calculated from the digitized LWD. The

digitized LWD area layer was used to extract the relevant extent of the DSM and DEM for each year. Volume of LWD were determined for water years 2017, 2019, and 2020 by calculating the surface difference between the DSM and DEM with the ArcGIS Pro 3D Analyst Tools (ArcGIS Pro 3.0.2, Esri, Redlands, California, USA).

3. Results

3.1. Geomorphic change

The difference of DEM (DoD) is a volumetric comparison between two surfaces. We compared annual surface conditions for 2016 through 2021 against the 2014 floodplain surface post excavation. Each year, floodplain wetting events influence the reconnected floodplain. Flood events were considered to be any flow event with discharge that exceeded $23 \text{ m}^3 \text{s}^{-1}$. Flood events for the period of study are listed in [Table 2](#) [76]. The duration and maximum discharge of each flood event are also provided.

The heterogeneous nature of annual wetting events is also expressed in the annual sediment dynamics across the reconnected floodplain in [Fig 5](#). In the DoDs at the top of [Fig 5](#), the erosion and deposition patterns in each DoD sequentially depict the formation of secondary channels, specific locations of sediment and debris, and multiple scours increasing at the northern-most section of the floodplain where flows begin to traverse the bank onto the floodplain.

DoD surfaces shown in [Figs 3](#) and [5](#) depict geomorphic change across the study area, and are supported by quantitative volumetric measurements of sediment change. For each study year, DEMs were compared to the 2014 year-zero surface. Net accretion, depletion, and change volumes were quantified for each surface comparison. Resulting net volumetric change are shown in [Table 3](#), and are restricted to the 2014 extent analyzed by Nichols and Viers [68]. Cumulative volumetric change began in 2016 with a net loss of more than $3,000 \text{ m}^3$ of sediment across the site but, after two additional years, more than $20,000 \text{ m}^3$ of additional sediment was measured in the 2014 to 2018 DoD. The maximum cumulative accretion since the 2014 baseline was in 2020 with almost $30,000 \text{ m}^3$. When the $1,718 \text{ m}^3$ of removed sediment is considered, the 2014 to 2020 accretion is $27,073 \text{ m}^3$ of new sediment within the original excavated area. Depletion rates varied between DoDs with the largest net loss of sediment measured between 2014 and 2016 at $3,250 \text{ m}^3$. When considering depletion, alone, the 2014 to 2021 DoD resulted in a $4,113 \text{ m}^3$ depletion of sediment, though the net change overall still accounted for $8,012 \text{ m}^3$ of sediment gained since 2014. Interannual values are much more varied. The interannual results do not consider year zero level ground, instead measuring only the variability within a given water year. Resulting vertical changes predominantly range from -1.5 meters to 1.5 meters in any one place, depicted in [Table 3](#) and [Fig 5](#).

The initial assessment of this site included projecting expected flow paths [68]. Those postulated channel delineations are replicated in [Fig 6A DEM 2014](#) (thick line) and compared to the 2014 channel center (dashed line). Since the 2015 study, annual elevation survey and DEM generation has facilitated quantification of surface differences and identification of secondary flow paths. [Fig 6B DEM 2017](#) and [6C DEM 2021](#) depict initial expectations of channel formation (thin line) overlaid with the realized secondary channel locations developed during 2017 and 2021 flow events (thick line).

The 2014 survey of the excavated site only allows for comparison across a limited section of the floodplain. However, in the near decade since, multiple floods have occurred sparking interest in the connected floodplain beyond the excavation. While the 2014 data set only allows for excavation site comparisons, the California Department of Water Resources, in conjunction with the National Oceanic and Atmospheric Association, surveyed the Sacramento-San

Table 2. Dates and max discharge flows (Q) by event and water year (WY) 2015–2021.

WY	Start Date	Days Exceeded	Max Q (cfs)	Max Q ($\text{m}^3 \text{s}^{-1}$)
WY15	2014–12–12	2	2,240	63.43
	2015–02–07	5	7,280	206.15
WY16	2015–12–22	3	4,190	118.65
	2016–01–06	1	930	26.33
	2016–01–18	9	2,240	63.43
	2016–01–30	6	5,840	165.37
	2016–02–18	2	1,190	33.7
	2016–03–05	27	9,180	259.95
	2016–04–09	4	1,150	32.56
	2016–04–23	1	1,030	29.17
WY17	2016–10–17	1	852	24.13
	2016–11–27	1	1,120	31.71
	2016–12–10	12	9,340	264.48
	2016–12–24	1	852	24.13
	2017–01–04	132	49,700	1,407.34
WY18	2017–11–16	2	1,390	39.36
	2018–01–09	2	2,090	59.18
	2018–03–03	1	1,530	43.32
	2018–03–13	43	22,500	637.13
WY19	2019–01–16	9	5,060	143.28
	2019–01–02	133	13,500	382.28
WY20	2019–12–07	3	1,630	46.16
	2020–03–15	5	5,210	147.53
	2020–04–05	26	7,180	203.31
	2020–05–18	2	844	23.90
WY21	2021–01–28	3	3,140	88.91
	2021–03–19	2	1,100	31.15

Table 2: Date and flow information for each event that exceeded the lowest floodplain wetting stage during the study period and the length of the high flow event. Length is the number of days that flows exceeded wetting stage at the Michigan Bar stream gage, or “Days Exceeded”. When comparing [Fig 2](#) to [Table 2](#), the individual pulses or ‘spikes’ in flow are not necessarily noted as individual flood events in [Table 2](#). These are ‘flood pulse events’ with only the max flow, or “Max Q”, of the largest pulse of a given flood event recorded here. Pulses generally take 18 to 24 hours to travel from Michigan Bar ([Fig 1A](#)) to the upper-most section of the study site. Images of inundation on select dates are provided in the [Figs A & B](#) in [S1 Text](#).

<https://doi.org/10.1371/journal.pwat.0000132.t002>

Joaquin Delta with Airborne LiDAR in 2007 [[107](#)], prior to any levee or floodplain modification, and provide public access to their resulting DEMs. Using this publicly available data set and the methods discussed above, [Fig 7A](#) depicts the sediment erosion and deposition along the excavated site and adjacent, reconnected floodplain in the DoD of 2021 compared to the 2007 landscape, when levees were intact. [Fig 7B](#) further articulates the change in channel formation by providing a cross section of the landscape following the red transect across [Fig 7A](#). The 2007 profile can be identified by the spikes in elevation that mark the levee elevations in grey.

3.2. Large wood

The sediment accretion and topographic heterogeneity beginning to form in 2017 (second DoD from the left in the top of [Fig 5](#)) that expands in each subsequent year is also the site of

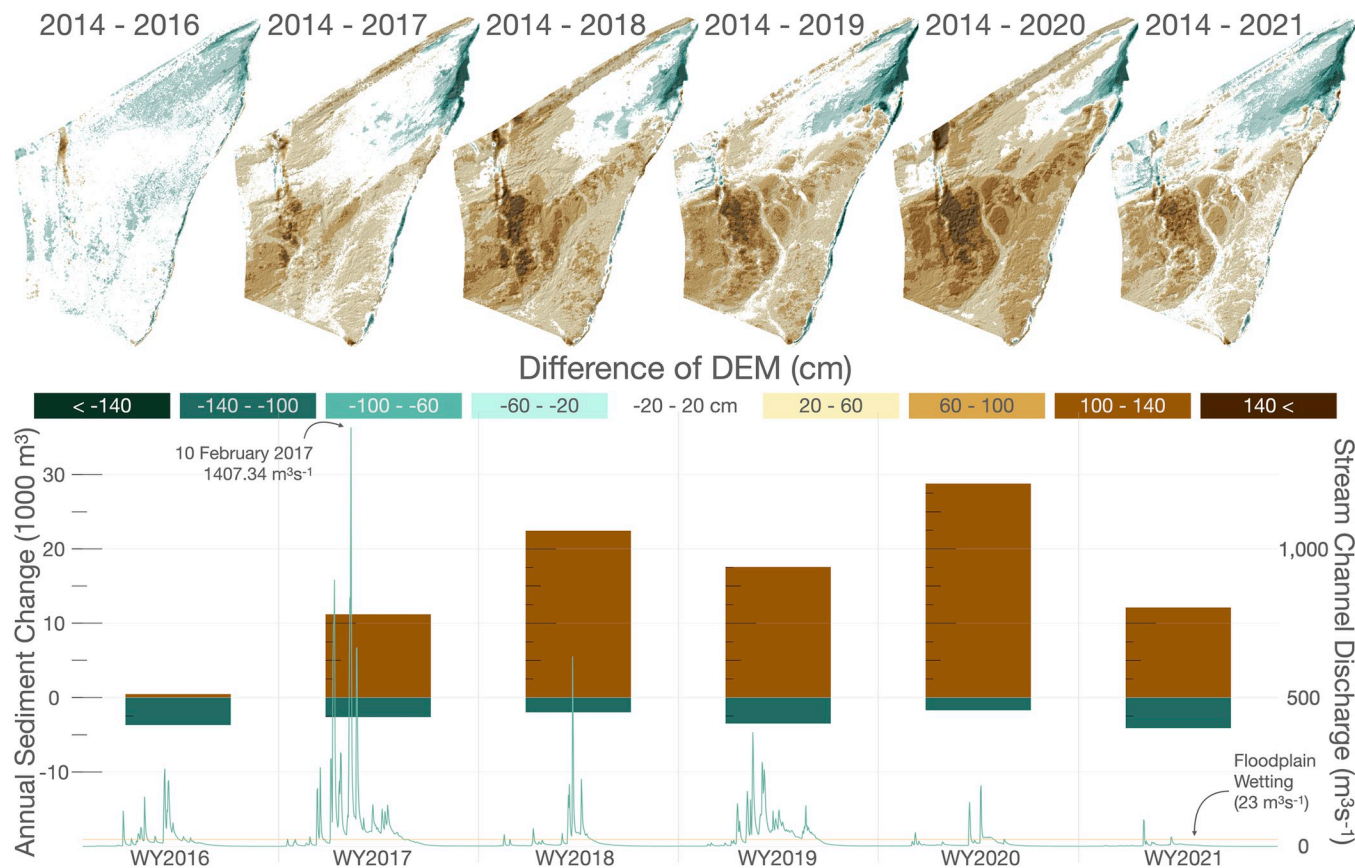


Fig 5. 2016 through 2021 annual comparison to 2014 DEM. 2016 through 2021 comparisons with 2014 (considered year zero) as difference of DEMs (DoD) with elevation change ranging in scale from -1.5 m to 1.5 m along the blue to vermilion color gradient aligning with the hydrograph for the Cosumnes River from 2016 through 2021. Each spike over the floodplain activation line (the gold line at $23 \text{ m}^3 \text{s}^{-1}$) would influence the sediment and propagules as floodwaters flowed across the floodplain. Annual accretion rates are depicted parallel to their annual timeline. The figure comparing interannual DoDs is available in the Fig H in S1 Text.

<https://doi.org/10.1371/journal.pwat.0000132.g005>

Table 3. Difference of DEM volume measurements.

2014 compared to:	2016	2017	2018	2019	2020	2021
Accretion (m^3)	457	11,207	22,458	17,575	28,791	12,125
Depletion (m^3)	-3,707	-2,630	-1,986	-3,502	-1,718	-4,113
Net Change (m^3)	-3,250	8,577	20,472	14,073	27,073	8,012
Interannual DoD:	2016: 2017	2017: 2018	2018: 2019	2019: 2020	2020: 2021	
Accretion (m^3)	15,903	10,276	2,088	12,096	525	
Depletion (m^3)	-1,454	-389	-7,457	-397	-19,534	
Net Change (m^3)	14,449	9,887	-5,369	11,699	-19,009	

Table 3: The net detectable volume difference, depletion, and accretion within the area of interest in m^3 for each monitored year compared to 2014 (year zero). In the top rows, ‘2014 compared to’, each column should be considered with reference of time between 2014 and the given column year rather than one column to another. The value in a given column is the total change between 2014 and that year (i.e. 2018 is the total change after 2015, 2016, 2017, and 2018 compared to the 2014 baseline). ‘Interannual DoD’ values are the DoD for each set of years listed. Unlike the top rows, which account for all change between the leveled excavation and the selected year, these DoDs are only from a single year to the next year. Caution must be taken to interpret the top three rows as the total accrued value up to the specified year while the bottom rows lack a baseline value.

<https://doi.org/10.1371/journal.pwat.0000132.t003>

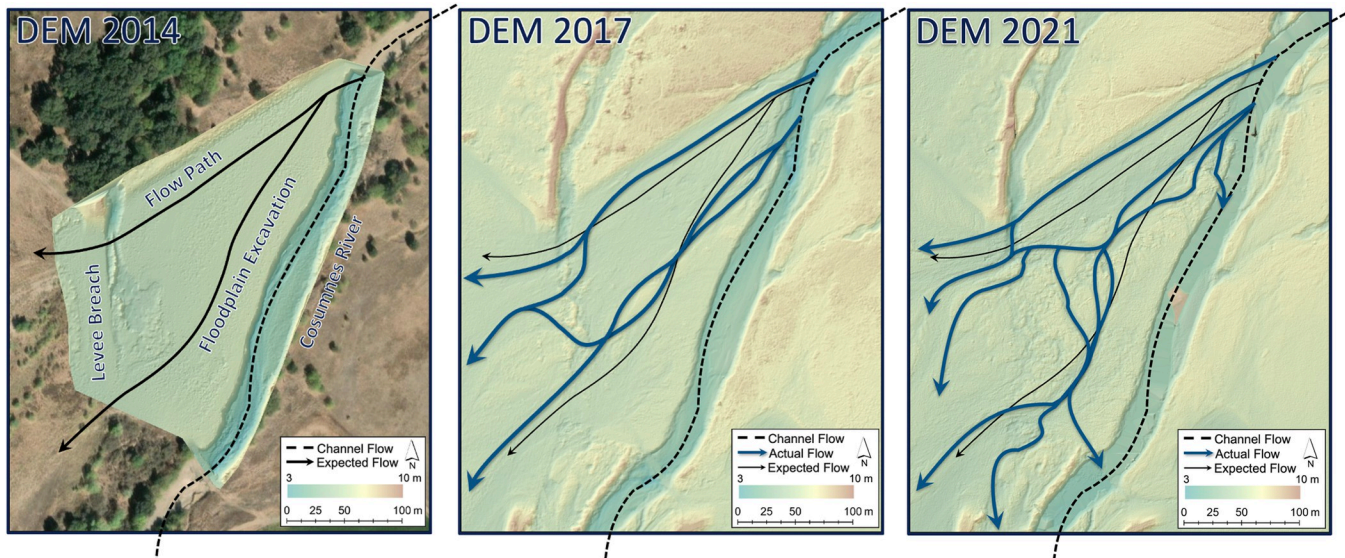


Fig 6. Flow path and alteration compared to Nichols & Viers 2017. 2014 DEM and flow path expectations post-reconnection as put forth by Nichols and Viers (2017) based on Florsheim and Mount (2002), followed by the resulting path dynamics apparent in the 2017 DEM and the 2021 DEM. Bold lines in A are the original flow path lines hypothesized and presented [35, 68]. B adapts the original projection to indicate the path flows followed (bolded blue line) in the 2017 LiDAR survey compared to the original projection (narrow black lines). In a similar fashion, C indicates the flow paths present in 2021 (in bolded blue lines) according to the 2021 DEM compared to the 2014 projection (narrow black lines).

<https://doi.org/10.1371/journal.pwat.0000132.g006>

extensive large wood (LWD) recruitment. A major deposit also forms through the DoDs in **Fig 5** at the base of the southern junction of the crevasse and the channel. After identification of LWD deposition, delineation of patches within the study site shown in **Fig 4** resulted in LWD extents of 627 m², 2,804 m², and 5,354 m² for 2017, 2019, and 2020 surveys respectively. Volumetric measures of LWD patches were 2,080, 7,807, and 22,234 m³ in 2017, 2019, and 2020. The accumulation of LWD in lateral positions, as depicted in **Fig 4**, corresponds to the conceptual framework presented by Nichols and Viers (2017) wherein LWD accumulates along emerging lateral levees of crevasse splays [80].

4. Discussion

In the original study design, Nichols & Viers (2017) hypothesized that as sand splay and crevasse splay complexes formed and expanded, sediment and LWD would deposit toward the channel progressively forming a lateral levee [68]. Following Florsheim and Mount (2002), who focused on a series of levee breaches further downstream from this study site (see southern extent of **Fig 1B** and **Table 1**), Nichols and Viers (2017) were only able to assess initial splay complex and lateral levee development in 2015 [68]. Subsequent flood pulse events have driven greater geomorphological evolution across the excavated site, depicted in **Figs 3–5**, extending the geomorphic evolution across the reconnected floodplain, as depicted in **Fig 7A**.

Hydrology during the study period was representative of extremes (**Table 2**). Discharge at the MHB gage ranged from 0 m³s⁻¹ (July 26–October 11, 2014; August 6–October 21, 2015; and August 1–September 22, 2021) to 1407.35 m³s⁻¹ (February 10, 2017; 2nd in **magnitude since 1907**), with 27 separate flood events that exceeded daily average flows greater than 23 m³s⁻¹. These flood events lasted from 1 to 133 days in duration, for a total of 438 days of flooding during the study period.

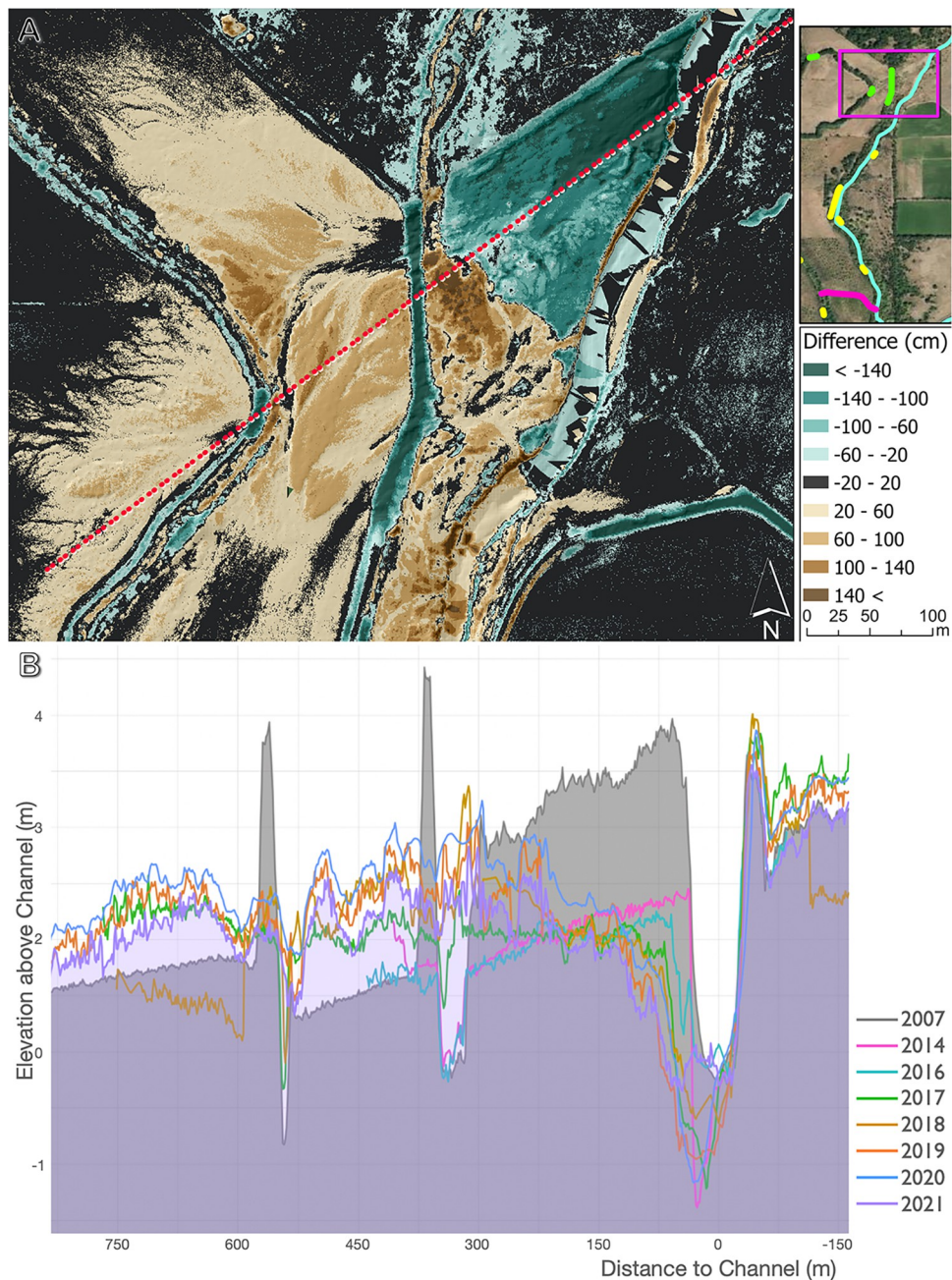


Fig 7. 2007 to 2021 DoD and synthesized cross-section profile. A: 2007 DEM with pre-excavation levees present compared to the 2021 DEM. Most change occurs within the -1.5 to 1.5 meter range. The area excavated in 2014 is boldly visible because of the continuous area of accretion. The perforated red line depicts the cross-section location further described in the B profile of each DEM available for 2007, 2014, and 2016 through 2021. The distinct levee features, both the levee and landscape adjacent to the channel and the levee further into the landscape, are prominent in the 2007 profile. The 2014 profile provides a visual of the leveling performed while each subsequent year conveys the various degrees of alteration across the excavated site and reconnected floodplain.

<https://doi.org/10.1371/journal.pwat.0000132.g007>

4.1. Geomorphic evolution

Geomorphic evolution of the restoration site is shown in [Fig 5](#), which compares 2014 floodplain surface conditions to subsequent years, indicating dynamic geomorphic surface changes correlated with flood events from variable water year conditions. For the 2014 to 2016 time period, [Fig 5](#) depicts minimal sediment deposition and much higher erosion for a total net change of $-3,250 \text{ m}^3$ ([Table 3](#)). Given that the site was only one water year removed from its excavation and leveling in 2016, the lack of established vegetation and geomorphic structure resulted in low surface roughness (inundated conditions on March 22, 2016, can be found in [Fig A](#) in [S1 Text](#)). These conditions likely resulted in high water velocity and increased shear stress during flow events, resulting in suspended sediment transport and erosion, given the small particle size dominance of this reach [108]. The location where deposition was observed included a rapid change in elevation and channel inflow (depicted in [Figs 3–5](#)), likely resulting in turbulent mixing, allowing for the sediment deposition depicted in the northeast region of the 2014 to 2016 DoD presented in [Fig 5](#).

During water year 2017, flows exceeded $1,400 \text{ m}^3 \text{s}^{-1}$ ([Fig 2](#) and [Table 2](#)) and floodwaters fully inundated the excavation site and reconnected floodplain for 128 days (inundated conditions on May 3, 2017, are documented in Supporting Material). Flows prior to WY17 exceeded $250 \text{ m}^3 \text{s}^{-1}$ once in WY16 ([Table 2](#)); however, like events preceding the 2016 DEM, most previous flood events were under $100 \text{ m}^3 \text{s}^{-1}$, with minimal potential for sediment deposition, natural recruitment, or LWD build-up. In the 2014 to 2017 DoD comparison in [Fig 5](#), erosional features measured 1 m to more than 1.4 m, but also exhibited high accretion (0.2 to more than 1.4 m) in the southwestern corner of the study site. The spatial distribution of scour and deposition remains across all later DoDs. The first geomorphic signs of lateral levee formation are visible in 2017, with secondary channels starting to develop (as shown in [Fig 6](#)). The DoD between 2016 and 2017 ([Fig H](#) in [S1 Text](#)) shows a similar deposition pattern and had a net sediment accumulation of $14,450 \text{ m}^3$. For the period from 2014 to 2017, LWD accumulated over 627 m^2 with a volume of $2,080 \text{ m}^3$.

In the 2014 to 2018 DoD, sediment accretion exceeded $22,000 \text{ m}^3$ ([Table 3](#)). Flood events in 2018 were modest with the $637.13 \text{ m}^3 \text{s}^{-1}$ peak daily discharge and a maximum 43-day duration flood event ([Table 2](#)). Erosional features extended from the cutbank feature in the northeast corner, but the majority of the site underwent deposition ([Fig 5](#)). An elongated region of non-uniform sediment deposition extends from the channel in the west-southwest direction across the site. Other studies have found similar areas of non-uniform sediment deposition to lead to secondary channels or flow paths [35]. In the 2017 to 2018 DoD ([Fig H](#) in [S1 Text](#)), there was a net accumulation of $9,890 \text{ m}^3$ across the excavation site.

Water year 2019 had longer flood duration than previous years (133 days) across 15 flood pulses, though peak flow never exceeded $400 \text{ m}^3 \text{s}^{-1}$ ([Table 2](#)). Sediment accretion volume was greater than $17,500 \text{ m}^3$, with spatial variation in depositional patterns along the west-southwest lateral levee. Secondary channel features in the 2014 to 2019 DoD shown in [Fig 5](#) are more pronounced compared to those in [Fig 6B](#). The erosion patterns at the cutbank expanded further onto the floodplain, accompanied by increased scouring (depletion volume since 2014 is more than $3,500 \text{ m}^3$), thereby reinforcing the development of secondary flow paths between 2017 and 2021 in [Fig 6](#). Sinuous channels begin to appear in the DoD as a result of sediment dynamics between WY17 and WY19. Net sediment change was $6,000 \text{ m}^3$ less between 2014 and 2019 compared to the DoD results between 2014 and 2018. The DoD between 2018 and 2019 resulted in a net loss of $5,370 \text{ m}^3$, verifying the reduction in cumulative sediment from 2014 to 2019 DoD. Field site observation and collected data verify the extended crevasse splay complex, the $7,807 \text{ m}^3$ of LWD, and the additional $14,073 \text{ m}^3$ of sediment deposits within the 2014 to 2019 DoD.

In water year 2020, flood pulses facilitated the largest accretion measurements compared to 2014 yet at nearly 29,000 m³ (Table 3 and Fig 5) with max discharge reaching only 203 m³s⁻¹ (Table 2). The longest wetted period was 26 days, additional information is provided in Table 2. Flows also occurred much later, compared to January in 2017 and 2019 or March in 2016 and 2018. Areas of deposition in previous DoDs display markedly increased cumulative volumes across the excavated site in the 2014 to 2020 DoD with the center area measuring 140 cm or more of deposition. Erosion measured at the channel is also less than in previous DoDs, a pattern that is reasonable with higher deposition. Later floodplain wetting flows that are smaller and less powerful may have resulted in a swift decline of carrying capacity as flows traversed the cutbank and velocity decreased. Results confirm 22,234 m³ of LWD in 2020 while multispectral data used for LWD also confirm propagule recruitment, both of which could decrease flow velocity drastically. When GCD between 2019 and 2020 was assessed (Table 3), there was 11,700 m³ of sediment added. During field site visits, in 2020, the floodplain beyond the study site (extent of Fig 7A) remained similar to WY2019, though the study site (extent of Figs 3–6) was much changed, indicating sediment deposits during WY2020 remained primarily within the study site.

Water year 2021 was the most water limited with only two flow events high enough to wet the floodplain, neither more than 90 m³s⁻¹. In the 2014–2021 DoD, the erosion along the cutbank that had been somewhat filled in the previous year expanded to extend more than 150 m onto the floodplain (Fig 5). Additionally, though the area does not depict erosion via a negative value or when considered alone, when compared to the deposition in the previous DoDs, the area north of the willows displays much lower deposition than all DoDs except the 2014 to 2016 (see Fig 5). Similarly, the southeastern region between the channel and developing lateral levee, expresses marked absence of prior deposition. The secondary channel east of the center willow patch is more defined as are several potential channels through the lateral levee formation and the west edge of the study site. These impacts of wetting events in WY2021 may be due to the small flood pulses with short residence time, 5 days total for the water year (see Table 3). As this comparison is between 2014 and 2021, there is a net accumulation of 8,012 m³ since 2014. However, when 2020 is compared to 2021, there is a net loss of 19,010 m³ validating the areas of removed deposition when comparing 2014–2021 DoDs to previous DoDs. The flood waters may have been able to reach the floodplain, but it appears that they quickly drained off the site and excised sediment with them. A similar phenomenon has been documented by Kondolf (1997) known as ‘hungry water’ [109]. Upon field inspection, the erosion quantified in the DoD aligns with visual assessments along with the identification of extensive LWD added.

The geomorphic evolution shaping the excavated landscape through time facilitated features such as sediment deposits, propagule recruitment, and LWD deposition. The variable and concentrated locations of such features have resulted in a heterogeneous landscape, even within the limited extent of the study site. Ultimately, the resulting heterogeneity across the excavation site in each DoD is only a small extent of the floodplain reconnected. With access to public data prior to the site becoming integrated into the Cosumnes River Preserve and levee manipulation, we directly compare current geomorphic characteristics to those in 2007, the most recent DEM publicly available. In Fig 7A, the sand splays and additional sediment deposits are visible in this 2007 to 2021 DoD. There was no land manipulation on the reconnected floodplain, only between the levee and the channel and the levee itself, within the study site depicted in previous figures. The excavated levee section and full extent of the excavated site are visible. The area excavated would appear as a uniform level of erosion in 2014, but various sand splays and deposits reduce those erosion or loss values with varying intensity. The area of highest deposition in Fig 7A provides the extent of willows that seem to have heavily contributed to the surrounding sediment dynamics (detailed annotations are also provided in Fig I in S1 Text). The profile of 2007 (with levee), 2014 (year of excavation), and 2016–2021

(years covered in this study), in [Fig 7B](#), provide further context to the evolution of the channel, excavated landscape, and former working land through time.

Many of the resulting features were originally postulated by Nichols and Viers (2017) or suggested in previous works such as Florsheim and Mount (2002). For example, the initial area of erosion at the cutbank that extended onto the floodplain is indicative of the scouring postulated by Florsheim and Mount (2002) that would expand to a secondary channel and accompanying lateral levees. Nichols and Viers (2017) then expanded the hypothesis suggesting that multiple sand splays, rather than a single lobe, would form and overlap. [Fig 7A](#) confirms the existence of multiple sand splay lobes and diverse sediment deposit characteristics. They also hypothesized that LWD would deposit and form a large lateral levee, increasing sediment deposition and driving further natural levee expansion. The existing lateral levee follows below the red hatched line across [Fig 7A](#) in the previously excavated area.

The hypothesized lateral levee of LWD and deposited sediment has since been realized in the excavated site from the channel to the willows (LWD: [Fig 4](#); Sediment: [Figs 3, 5](#) and [7](#)). When Nichols and Viers (2017) postulated that the larger levee excavation would produce multiple sand splay lobes and crevasse splay complexes, there was not a willow patch hindering splay formation or additional levees impeding or concentrating flows further down the floodplain [68]. We cannot postulate what the outcome would have been had the willows been removed at the time of excavation, but our results provide the context in which various splays have formed since the excavation.

4.2. Large wood accumulation

In [Fig 4](#), LWD is scattered laterally along the channel and then extends onto the floodplain perpendicular to the channel. As the number of wetting events has increased through time, LWD has grown from no deposition to covering more than 5,000 m² across the excavated landscape and directly adjacent areas, including a large log jam at the cutbank. The area of LWD in [Fig 4](#) aligns with the areas of highest deposition in [Fig 3](#) and throughout [Fig 5](#). Such consistent distribution of LWD with high sediment deposition indicates a positive relationship between the deposit types (see [Fig I](#) in [S1 Text](#)). Some areas within the study site provide more clarity on this relationship, such as the lateral levee forming via increased sediment and LWD deposition. Areas of correlated deposition align with the findings of other studies, such as Abbe and Montgomery (1996) who documented LWD providing refugia for propagule deposition and refugia for the development of riparian forest or Wohl and Scott (2017) who determined that sediment accumulation positively correlates with LWD volume [110, 111]. Such a positive correlation may be driven by LWD increasing surface roughness which could support sediment and propagule deposition. Evidence exists in [Figs 3–5](#) to support propagule recruitment or deposition in areas of high sediment accretion. Converse to this point of aligned deposition is the cutbank where erosion slowly extends onto the floodplain in [Fig 5](#). That area is also the site of an extensive log jam (northernmost area in [Fig 4](#) and highlighted in Supporting Material). As the log jam has grown, so has the volume of erosion at the cutbank, more than 1.5 m of erosion (see the area of highest erosion in [Fig 3](#)). This erosion is also found in [Fig 7B](#) where the channel is progressively expanding west-southwest toward the floodplain. Such findings are paralleled in other rivers where log jams may allow for sediment erosion but prevent complete bank destabilization [111], as has been recorded here since the log jam began development in 2017.

4.3. Applicability to other river systems

Multi-benefit floodplain restoration as NbS offers a balanced approach for managing large river floodplains for ecological and human interests [50]. In the Sacramento-San Joaquin

Delta region, including the Cosumnes River study site, flood resilience has increased by integrating ecological restoration with flood management [112], despite implementation challenges such as land acquisition, funding, and regulatory hurdles. On a global scale, other large river systems are trying to achieve climate resilience given recent hydroclimatic extremes. For example, in the USA, the Mississippi River experienced its longest flooding period on record in 2019 [113]. Similarly, in July 2021, Europe faced historic flooding challenges [114]. While river stage set contemporary records in the Netherlands along the Rhine and Meuse Rivers into the Rhine-Meuse-Scheldt delta, flood waters did not breach into urban areas or critical infrastructure along the Rhine and caused comparatively limited damage along the Meuse, primarily to the province of Limburg adjacent to the Belgium-Netherlands border [115]. This was in stark contrast to the deadly flooding experienced upstream on the Ahr River, a tributary of the Rhine River, through Germany and the Meuse River through Belgium [116]. A significant component of the Netherlands' flood management strategy is the "Room for the River" project with strategic setback levees, expanded floodplains, and structural riverbed modifications [117]. By creating more space within the floodplain to reduce the peak flood stage downstream and facilitate faster drainage away from urban areas during high water levels, this innovative design ensured that rivers like the Rhine and Meuse had ample room to expand [24, 118].

Further insights from global practices in river systems like the Tisza [119], Dijle [120], and Murray-Darling [121] underscore the importance of restoring natural habitats as a foundational element of their NbS strategies. A recurring theme across these and other regions is the challenge and necessity of balancing human needs, such as agriculture and urban development, with environmental conservation [118]. The dynamic nature of river systems, compounded by the uncertainties of climate change, emphasizes the importance of adaptive management, which involves ongoing monitoring and the flexibility to adjust strategies based on evolving conditions and new insights. Collectively, the experiences from Sacramento-San Joaquin, the Rhine-Meuse-Scheldt, and other global river systems highlight both the potential benefits and inherent complexities of multi-benefit restoration in river floodplains aimed at providing Nature-based Solutions to flooding, emphasizing its relevance in diverse geographical and climatic contexts.

5. Conclusions

This study builds on more than two decades of published research investigating process-based restoration approaches via levee manipulation along the Cosumnes River in California, USA [79]. With its natural flow regime signature, episodic and unregulated flood events, and adjacent floodplains, the Cosumnes River is uniquely positioned to study experimental NbS to flooding. We evaluated the geomorphic response when a NbS was implemented. A 250-meter section of levee along the Cosumnes River within CRP was excavated and annual DEMs were compared to measure annual accretion rates, deposition volume, and determine the presence and extent of LWD post-reconnection. Because of the natural flow regime of the Cosumnes River, this research includes heterogeneous water years and flow events producing heterogeneous results within each DoD comparison.

Initial conceptual models postulated that upon breaching the levee, flows would scour at the bank and lead to various morphological changes. However, as floodplain research progressed, it was hypothesized that the width of the levee breach would influence floodplain response, potentially facilitating large wood and debris deposition to create a lateral levee along the channel. Though there were limited initial findings of a crevasse and minimal sand splay formation in the 2015 study, the results found here support the initial expectation of overlapping sand splays, which now extend more than 700 m from the channel down the

reconnected floodplain. Large wood has been deposited in a levee located laterally to the main channel. This wood has initiated secondary channel flow paths both along sand splays and through LWD deposits.

The implications of LWD and heterogeneous outcomes extend to habitat formation and propagule recruitment. Native cottonwoods are propagating within the sand splays as well as at the terminal region of the floodplain more than 1,000 m south of the excavation (Clifton et al. in prep and documented in **Fig J** in [S1 Text](#)). Sediment accretion and native recruitment serve as two key indicators of functionality, enhanced by reconnected flows. Ultimately, these floodplain processes form the foundation for a functional riparian corridor. While this river system faces numerous anthropogenic impacts, the results of this study show that sediment transport, expressed through sand splay and crevasse complex formation, occurs within the first few years of high flows. LWD deposition increases as surface roughness rises, and native plants propagate when lateral connectivity is restored, allowing floodwaters to once again reside in their floodplains. The outcomes observed in this river, characteristic of a natural flow regime in a Mediterranean-montane climate, are relevant to rivers in California and other regions with similar climatic conditions.

In an era where climate change and anthropogenic impacts pose escalating challenges to sustaining Earth, multi-benefit floodplain restoration as a nature-based solution to both reducing flood risk and improving ecosystem functioning is essential. This study provided additional evidence that strategic interventions in river systems can lead to dynamic hydrogeomorphic changes which play pivotal roles in habitat formation and species recruitment. Such outcomes serve ecological purposes simultaneously with tangible benefits in flood risk mitigation by attenuating floodwaters and diminishing peak flows. The long-term monitoring of this study site provides compelling evidence for the potential and efficacy of NbS in addressing the pressing need for win-win outcomes in ecosystem management.

Study site access required an annual General Access Permit with The Nature Conservancy through the Cosumnes River Preserve staff, which required annual renewal. This process provided general research access for properties managed by CRP including those areas owned by other agencies. Each person also submitted an individual Release Form acknowledging the limitations of use and access granted by CRP. Each site visit also required an itinerary and confirmation of access for each property included within the itinerary from CRP as well as safety protocols from both CRP and the University of California, Merced.

Supporting information

S1 Text.

(PDF)

Acknowledgments

This work is based on nearly four decades of research by many researchers and their teams, to which we extend our gratitude. We are grateful to A Rallings, M Kalua, A Anderson, L Booth, B Stark, and F Gamino who supported field work campaigns, permitting and access, data collection, management, and processing as well as E Hestir and others who provided valuable feedback. We thank Sara Sweet and the staff at The Nature Conservancy, California Department of Fish & Wildlife, and the Bureau of Land Management for study site access.

Author Contributions

Conceptualization: Britne Clifton, Joshua H. Viers.

Data curation: Britne Clifton, Joshua H. Viers.

Formal analysis: Britne Clifton.

Funding acquisition: Joshua H. Viers.

Investigation: Britne Clifton.

Methodology: Britne Clifton, Joshua H. Viers.

Project administration: Britne Clifton, Joshua H. Viers.

Resources: Joshua H. Viers.

Software: Britne Clifton.

Supervision: Britne Clifton, Joshua H. Viers.

Validation: Britne Clifton.

Visualization: Britne Clifton.

Writing – original draft: Britne Clifton.

Writing – review & editing: Britne Clifton, Joshua H. Viers.

References

1. Naiman RJ, Decamps H, Pollock M. The Role of Riparian Corridors in Maintaining Regional Biodiversity. *Ecological Applications*. 1993; 3(2):209–12. <https://doi.org/10.2307/1941822> PMID: 27759328
2. Tockner K, Stanford JA. Riverine Flood Plains: Present State and Future Trends. *Environmental Conservation*. 2002; 29(3):308–30. <https://doi.org/10.1017/S037689290200022X>
3. Ward JV, Tockner K, Schiemenz F. Biodiversity of floodplain river ecosystems: ecotones and connectivity. *Regulated Rivers: Research & Management*. 1999; 15(1–3):125–39. [https://doi.org/10.1002/\(sici\)1099-1646\(199901/06\)15:1/3<125::aid-rrr523>3.0.co;2-e](https://doi.org/10.1002/(sici)1099-1646(199901/06)15:1/3<125::aid-rrr523>3.0.co;2-e)
4. Dunne T, Aalto RE. Large River Floodplains: Elsevier Ltd.; 2013. 645–78 p.
5. Tockner K, Malard F, Ward JV. An extension of the flood pulse concept. *Hydrological Processes*. 2000; 14(16–17):2861–83. [https://doi.org/10.1002/1099-1085\(200011/12\)14:16/17<2861::AID-HYP124>3.0.CO;2-F](https://doi.org/10.1002/1099-1085(200011/12)14:16/17<2861::AID-HYP124>3.0.CO;2-F).
6. Mertes LAK, Daniel DL, Melack JM, Nelson B, Martinelli LA, Forsberg BR. Spatial patterns of hydrology, geomorphology, and vegetation on the floodplain of the Amazon river in Brazil from a remote sensing perspective. *Geomorphology*. 1995; 13(1–4):215–32. [https://doi.org/10.1016/0169-555X\(95\)00038-7](https://doi.org/10.1016/0169-555X(95)00038-7)
7. Kondolf GM, Piégay H. Tools in fluvial geomorphology 2005. 1–688 p.
8. Leopold LB, Wolman MG, Miller JP. Fluvial Processes in Geomorphology. 2nd ed. Mineola, New York: Dover Publishing Inc.; 2020.
9. Hupp CR, Osterkamp WR. Riparian vegetation and fluvial geomorphic processes. *Geomorphology*. 1996; 14:277–95.
10. Naiman RJ, Décamps H. The ecology of interfaces: Riparian zones. *Annual Review of Ecology and Systematics*. 1997; 28(102):621–58. <https://doi.org/10.1146/annurev.ecolsys.28.1.621>
11. Amoros C, Bornette G. Connectivity and biocomplexity in waterbodies of riverine floodplains. *Freshwater Biology*. 2002; 47(4):761–76. <https://doi.org/10.1046/j.1365-2427.2002.00905.x>
12. Verry ES, Dolloff CA, Manning ME. Riparian ecotone: A functional definition and delineation for resource assessment. *Water, Air, and Soil Pollution: Focus*. 2004; 4(1):67–94. <https://doi.org/10.1023/B:WAFO.0000012825.77300.08>
13. McInerney PJ, Stoffels RJ, Shackleton ME, Davey CD. Flooding drives a macroinvertebrate biomass boom in ephemeral floodplain wetlands. *Freshwater Science*. 2017; 36(4):726–38. <https://doi.org/10.1086/694905>
14. Opperman JJ, Moyle PB, Larsen EW, Florsheim JL, Manfree AD. Floodplains: Processes and Management for Ecosystem Services. Oakland, California: University of California Press; 2017.

15. Hayes DS, Brändle JM, Seliger C, Zeiringer B, Ferreira T, Schmutz S. Advancing towards functional environmental flows for temperate floodplain rivers. *Science of the Total Environment*. 2018; 633:1089–104. <https://doi.org/10.1016/j.scitotenv.2018.03.221> PMID: 29758861
16. Wohl E. Rivers in the Landscape 2020. 319–59 p.
17. Ward JV, Tockner K, Arscott DB, Claret C. Riverine landscape diversity. *Freshwater Biology*. 2002; 47(4):517–39. <https://doi.org/10.1046/j.1365-2427.2002.00893.x>
18. Gregory SV, Swanson FJ, McKee WA, Cummins KW. An Ecosystem Perspective of Riparian Zones. *BioScience*. 1991; 41(8):540–51. <https://doi.org/10.2307/1311607>
19. Wohl E. Spatial heterogeneity as a component of river geomorphic complexity. *Progress in Physical Geography*. 2016; 40(4):598–615. <https://doi.org/10.1177/0309133316658615>
20. Biron PM, Buffin-Bélanger T, Massé S. The need for river management and stream restoration practices to integrate hydrogeomorphology. *Canadian Geographer*. 2018; 62(2):288–95. <https://doi.org/10.1111/cag.12407>
21. Kuiper JJ, Janse JH, Teurlincx S, Verhoeven JTA, Alkemade R. The impact of river regulation on the biodiversity intactness of floodplain wetlands. *Wetlands Ecology and Management*. 2014; 22(6):647–58. <https://doi.org/10.1007/s11273-014-9360-8>
22. Grill G, Lehner B, Thieme M, Geenen B, Tickner D, Antonelli F, et al. Mapping the world's free-flowing rivers. *Nature*. 2019; 569(7755):215–21. <https://doi.org/10.1038/s41586-019-1111-9> PMID: 31068722
23. Costanza R, de Groot R, Braat L, Kubiszewski I, Fioramonti L, Sutton P, et al. Twenty years of ecosystem services: How far have we come and how far do we still need to go? *Ecosystem Services*. 2017; 28:1–16. <https://doi.org/10.1016/j.ecoser.2017.09.008>
24. Jakubínský J, Prokopová M, Raška P, Salvati L, Bezak N, Cudlín O, et al. Managing floodplains using nature-based solutions to support multiple ecosystem functions and services. *WIREs Water*. 2021; 8(5). <https://doi.org/10.1002/wat2.1545>
25. Mondal S, Patel PP. Examining the utility of river restoration approaches for flood mitigation and channel stability enhancement: a recent review. *Environmental Earth Sciences*. 2018; 77(5):1–25. <https://doi.org/10.1007/s12665-018-7381-y>
26. Dybala KE, Matzek V, Gardali T, Seavy NE. Carbon sequestration in riparian forests: A global synthesis and meta-analysis. *Global Change Biology*. 2019; 25(1):57–67. <https://doi.org/10.1111/gcb.14475> PMID: 30411449
27. Graf WL. Damage control: Restoring the physical integrity of America's rivers. *Annals of the Association of American Geographers*. 2001; 91(1):1–27. <https://doi.org/10.1111/0004-5608.00231>
28. Knox RL, Morrison RR, Wohl E. A river ran through it: Floodplains as America's newest relict landform. *Science Advances*. 2022; 8(25):1–6. <https://doi.org/10.1126/sciadv.abo1082> PMID: 35749493
29. Underwood EC, Hutchinson RA, Viers JH, Kelsey TR, Distler T, Marty J. Quantifying trade-offs among ecosystem services, biodiversity, and agricultural returns in an agriculturally dominated landscape under future land-management scenarios. *San Francisco Estuary and Watershed Science*. 2017; 15(2). <https://doi.org/10.15447/sfews.2017v15iss2art4>
30. Ga Tobin. The levee love affair: A stormy relationship? *Journal of the American Water Resources Association*. 1995; 31(3).
31. Wohl E, Angermeier PL, Bledsoe B, Kondolf GM, MacDonnell L, Merritt DM, et al. River restoration. *Water Resources Research*. 2005; 41(10):1–12. <https://doi.org/10.1029/2005WR003985>
32. Wohl E. Forgotten Legacies: Understanding and Mitigating Historical Human Alterations of River Corridors. *Water Resources Research*. 2019; 55(7):5181–201. <https://doi.org/10.1029/2018WR024433>
33. Knox RL, Wohl E, Morrison RR. Levees don't protect, they disconnect: A critical review of how artificial levees impact floodplain functions. *Science of the Total Environment*. 2022; 837:155773–. <https://doi.org/10.1016/j.scitotenv.2022.155773> PMID: 35537517
34. Wing OJ, Bates PD, Smith AM, Sampson CC, Johnson KA, Fargione J, et al. Estimates of present and future flood risk in the conterminous United States. *Environmental Research Letters*. 2018; 13(3):034023. <https://doi.org/10.1088/1748-9326/aaac65>
35. Florsheim JL, Mount JF. Restoration of floodplain topography by sand-splay complex formation in response to intentional levee breaches, Lower Cosumnes River, California. *Geomorphology*. 2002; 44(1–2):67–94. [https://doi.org/10.1016/S0169-555X\(01\)00146-5](https://doi.org/10.1016/S0169-555X(01)00146-5)
36. Swenson RO, Whitener K, Eaton M. Restoring floods on floodplains: riparian and floodplain restoration at the Cosumnes River Preserve. *California Riparian Systems: Processes and Floodplain Management, Ecology, Restoration, 2001 Riparian Habitat and Floodplains Conference Proceedings*, Faber PM (ed) Riparian Habitat Joint Venture: Sacramento, CA. 2003;(April):224–9.

37. Opperman JJ, Galloway GE, Fargione J, Mount JF, Richter BD, Secche S. Sustainable Floodplains Through Large-Scale Reconnection to Rivers. *Science*. 2009; 326(December):1487–8.
38. Larsen EW, Girvetz EH, Fremier AK. Assessing the effects of alternative setback channel constraint scenarios employing a river meander migration model. *Environmental Management*. 2006; 37(6):880–97. <https://doi.org/10.1007/s00267-004-0220-9> PMID: 16456633
39. Smith DL, Miner SP, Theiling CH, Behm R, Nestler JM. Levee Setbacks: An Innovative, Cost-Effective, and Sustainable Solution for Improved Flood Risk Management. Washington, DC: 2017.
40. Palmer MA, Bernhardt ES, Allan JD, Lake PS, Alexander G, Brooks S, et al. Standards for ecologically successful river restoration. *Journal of Applied Ecology*. 2005; 42(2):208–17. <https://doi.org/10.1111/j.1365-2664.2005.01004.x>
41. Beechie TJ, Sear DA, Olden JD, Pess GR, Buffington JM, Moir H, et al. Process-based principles for restoring river ecosystems. *BioScience*. 2010; 60(3):209–22. <https://doi.org/10.1525/bio.2010.60.3.7>
42. Kondolf GM. Setting goals in river restoration: When and where can the river "heal itself"? *Geophysical Monograph Series*. 2011; 194:29–43. <https://doi.org/10.1029/2010GM001020>
43. Ciotti D, McKee J, Pope K, Kondolf GM, Pollock M. Process-based design criteria for restoring fluvial systems. *BioScience*. 2020.
44. Skidmore P, Wheaton J. Riverscapes as natural infrastructure: Meeting challenges of climate adaptation and ecosystem restoration. *Anthropocene*. 2022; 38(February 2021):100334–. <https://doi.org/10.1016/j.ancene.2022.100334>
45. Cohen-Shacham E, Andrade A, Dalton J, Dudley N, Jones M, Kumar C, et al. Core principles for successfully implementing and upscaling Nature-based Solutions. *Environmental Science and Policy*. 2019; 98:20–9. <https://doi.org/10.1016/j.envsci.2019.04.014>
46. Serra-Llobet A, Jähnig SC, Geist J, Kondolf GM, Damm C, Scholz M, et al. Restoring Rivers and Floodplains for Habitat and Flood Risk Reduction: Experiences in Multi-Benefit Floodplain Management From California and Germany. *Frontiers in Environmental Science*. 2022; 9(March):1–24. <https://doi.org/10.3389/fenvs.2021.778568>
47. Sowińska-Świerkosz B, García J. What are Nature-based solutions (NBS)? Setting core ideas for concept clarification. *Nature-Based Solutions*. 2022; 2(May 2021):100009. <https://doi.org/10.1016/j.nbsj.2022.100009>
48. Walters GM. Nature-based solutions to address global societal challenges 2016.
49. FEMA. Engineering With Nature 2011. 3–33 p.
50. Van Rees CB, Jumani S, Abera L, Rack L, McKay SK, Wenger SJ. The potential for nature-based solutions to combat the freshwater biodiversity crisis. *PLOS Water*. 2023; 2(6):e0000126. <https://doi.org/10.1371/journal.pwat.0000126>
51. Florsheim JL, Mount JF. Changes in lowland floodplain sedimentation processes: Pre-disturbance to post-rehabilitation, Cosumnes River, CA. *Geomorphology*. 2003; 56(3–4):305–23. [https://doi.org/10.1016/S0169-555X\(03\)00158-2](https://doi.org/10.1016/S0169-555X(03)00158-2)
52. Mount JF, Florsheim JL, Trowbridge WB. Restoration of Dynamic Floodplain Topography and Riparian Vegetation Establishment Through Engineered Levee Breaching. *International Association of Hydrological Sciences*. 2002; 276:85–91.
53. Dierauer J, Pinter N, Remo JWF. Evaluation of levee setbacks for flood-loss reduction, Middle Mississippi River, USA. *Journal of Hydrology*. 2012;450–451:1–8. <https://doi.org/10.1016/j.jhydrol.2012.05.044>
54. Seavy NE, Gardali T, Golet GH, Griggs FT, Howell CA, Kelsey R, et al. Why climate change makes riparian restoration more important than ever: Recommendations for practice and research. *Ecological Restoration*. 2009; 27(3):330–8. <https://doi.org/10.3368/er.27.3.330>
55. Nelson EJ, Kareiva P, Ruckelshaus M, Arkema K, Geller G, Girvetz E, et al. Climate change's impact on key ecosystem services and the human well-being they support in the US. *Frontiers in Ecology and the Environment*. 2013; 11(9):483–93. <https://doi.org/10.1890/120312>
56. Liao KH. From flood control to flood adaptation: A case study on the Lower Green River Valley and the City of Kent in King County, Washington. *Natural Hazards*. 2014; 71(1):723–50. <https://doi.org/10.1007/s1069-013-0923-4>
57. Fischer J, Lindenmayer DB, Manning AD. Biodiversity, ecosystem function, and resilience: Ten guiding principles for commodity production landscapes. *Frontiers in Ecology and the Environment*. 2006; 4(2):80–6. [https://doi.org/10.1890/1540-9295\(2006\)004\[080:BEFART\]2.0.CO;2](https://doi.org/10.1890/1540-9295(2006)004[080:BEFART]2.0.CO;2)
58. Davies PM. Climate change implications for river restoration in global biodiversity hotspots. *Restoration Ecology*. 2010; 18(3):261–8. <https://doi.org/10.1111/j.1526-100X.2009.00648.x>

59. Tockner K, Pusch M, Borchardt D, Lorang MS. Multiple stressors in coupled river-floodplain ecosystems. *Freshwater Biology*. 2010; 55(SUPPL. 1):135–51. <https://doi.org/10.1111/j.1365-2427.2009.02371.x>
60. Sendek A, Kretz L, van der Plas F, Seele-Dilbat C, Schulz-Zunkel C, Vieweg M, et al. Topographical factors related to flooding frequency promote ecosystem multifunctionality of riparian floodplains. *Eco-logical Indicators*. 2021; 132:108312–. <https://doi.org/10.1016/j.ecolind.2021.108312>
61. Schindler S, Sebesvari Z, Damm C, Euller K, Mauerhofer V, Schneidergruber A, et al. Multifunctionality of floodplain landscapes: Relating management options to ecosystem services. *Landscape Ecology*. 2014; 29(2):229–44. <https://doi.org/10.1007/s10980-014-9989-y>
62. King J, Holmes R, Burkholder S, Holzman J, Suedel B. Advancing nature-based solutions by leveraging Engineering With Nature strategies and landscape architectural practices in highly collaborative settings. *Integrated Environmental Assessment and Management*. 2022; 18(1):108–14. <https://doi.org/10.1002/ieam.4473> PMID: 34101357
63. Dahl TE. Wetlands losses in the United States. US Department of the Interior, Fish and Wildlife Service, Washington, DC. 1990:21–.
64. Macfarlane WW, Gilbert JT, Gilbert JD, Saunders WC, Hough-Snee N, Hafen C, et al. What are the Conditions of Riparian Ecosystems? Identifying Impaired Floodplain Ecosystems across the Western U.S. Using the Riparian Condition Assessment (RCA) Tool. *Environmental Management*. 2018; 62(3):548–70. <https://doi.org/10.1007/s00267-018-1061-2> PMID: 29752496
65. Bernhardt ES, Palmer M, Allan JD, Alexander G, Barnas K, Brooks S, et al. Synthesizing US River Restoration Efforts. *Science*. 2005; 308(April):636–8.
66. Swenson RO, Reiner RJ, Reynolds M, Marty J. River Floodplain Restoration Experiments Offer a Window into the Past. In: Wiens JA, Hayward GD, Safford HD, Giffen CM, editors.: John Wiley & Sons, Ltd.; 2012. p. 218–31.
67. Dybala K, Dettling M, Gardali T, Grossman J, Kelsey R, Seavy N. Advancing ecological restoration through experimental design on spatial and temporal scales relevant to wildlife. 2017. <https://doi.org/10.7287/peerj.preprints.3365>
68. Nichols AL, Viers JH. Not all breaks are equal: Variable hydrologic and geomorphic responses to intentional levee breaches along the lower Cosumnes River, California. *River Research and Applications*. 2017; 33(7):1143–55. <https://doi.org/10.1002/rra.3159>
69. Dybala KE, Steger K, Walsh RG, Smart DR, Gardali T, Seavy NE. Optimizing carbon storage and biodiversity co-benefits in reforested riparian zones. *Journal of Applied Ecology*. 2019; 56(2):343–53. <https://doi.org/10.1111/1365-2664.13272>
70. Trowbridge WB, Anderson M, Mount JF. The influence of restored flooding on floodplain plant distribution 2002.
71. Whipple AA, Viers JH, Dahlke HE. Flood regime typology for floodplain ecosystem management as applied to the unregulated Cosumnes River of California, United States. *Ecohydrology*. 2017; 10(5):1–18. <https://doi.org/10.1002/eco.1817>
72. Booth EG, Mount JF, Viers JH. Hydrologic Variability of the Cosumnes River Floodplain. *San Francisco Estuary and Watershed Science*. 2006; 4(2). <https://doi.org/10.15447/sfews.2006v4iss2art2>
73. Esri, cartographer World Hillshade 2023.
74. Esri, cartographer USA State Boundaries 2021.
75. Esri, cartographer USA NAIP Imagery: Natural Color 2021.
76. NWIS Site Information for USA: Site Inventory [Internet]. U.S. Department of the Interior | U.S. Geological Survey. 2023. Available from: https://waterdata.usgs.gov/nwis/inventory/?site_no=11335000&agency_cd=USGS.
77. Florsheim JL, Mount JF, Constantine CR. A geomorphic monitoring and adaptive assessment framework to assess the effect of lowland floodplain river restoration on channel-floodplain sediment continuity. *River Research and Applications*. 2006; 22(3):353–75. <https://doi.org/10.1002/rra.911>
78. Whipple AA, Grossinger RM, Rankin D, Stanford B, Askevold RA. Sacramento-San Joaquin Delta Historical Ecology Investigation: Exploring Pattern and Process. Richmond, CA: Prepared for the California Department of Fish and Game and Ecosystem Restoration Program. A Report of SFEI-ASC's Historical Ecology Program, SFEI-ASC Publication #672, San Francisco Estuary Institute-Aquatic Science Center, 2012.
79. Fleckenstein JH, Anderson ML, Fogg GE, Mount JF. Managing surface water-groundwater to restore fall flows in the Cosumnes River. *Journal of Water Resources Planning and Management*. 2004; 130(4):301–10. [https://doi.org/10.1061/\(ASCE\)0733-9496\(2004\)130:4\(301\)](https://doi.org/10.1061/(ASCE)0733-9496(2004)130:4(301)).

80. Vasco DW, Farr TG, Jeanne P, Doughty C, Nico P. Satellite-based monitoring of groundwater depletion in California's Central Valley. *Scientific Reports*. 2019; 9(1):1–14. <https://doi.org/10.1038/s41598-019-52371-7> PMID: 31690776
81. Young CA, Escobar-Arias MI, Fernandes M, Joyce B, Kiparsky M, Mount JF, et al. Modeling the Hydrology of Climate Change in California's Sierra Nevada for Subwatershed Scale Adaptation1. *JAWRA Journal of the American Water Resources Association*. 2009; 45(6):1409–23. <https://doi.org/10.1111/j.1752-1688.2009.00375.x>
82. Rhoades AM, Jones AD, Ullrich PA. The Changing Character of the California Sierra Nevada as a Natural Reservoir. *Geophysical Research Letters*. 2018; 45(23):13,008–13,19. <https://doi.org/10.1029/2018GL080308>
83. Larsen Wurlzel Associates I. Reclamation District No. 800 Operations and Maintenance Assessment Final Engineer's Report. Sacramento, CA: 2018.
84. The Nature Conservancy. Cosumnes River Preserve Revised Management Plan. TNC Cosumnes River Preserve, 2022.
85. Jeffres CA, Opperman JJ, Moyle PB. Ephemeral floodplain habitats provide best growth conditions for juvenile Chinook salmon in a California river. *Environmental Biology of Fishes*. 2008; 83(4):449–58. <https://doi.org/10.1007/s10641-008-9367-1>
86. Seavy NE, Viers JH, Wood JK. Riparian bird response to vegetation structure: A multiscale analysis using LiDAR measurements of canopy height. *Ecological Applications*. 2009; 19(7):1848–57. <https://doi.org/10.1890/08-1124.1> PMID: 19831074
87. Ogaz MH, Rypel AL, Lusardi RA, Moyle PB, Jeffres CA. Behavioral cues enable native fishes to exit a California floodplain while leaving non-native fishes behind. *Ecosphere*. 2022; 13:1–18. <https://doi.org/10.1002/ecs2.4293>
88. Ahearn DS, Viers JH, Mount JF, Dahlgren RA. Priming the productivity pump: Flood pulse driven trends in suspended algal biomass distribution across a restored floodplain. *Freshwater Biology*. 2006; 51(8):1417–33. <https://doi.org/10.1111/j.1365-2427.2006.01580.x>
89. Steger K, Fiener P, Marvin-DiPasquale M, Viers JH, Smart DR. Human-induced and natural carbon storage in floodplains of the Central Valley of California. *Science of the Total Environment*. 2019; 651:851–8. <https://doi.org/10.1016/j.scitotenv.2018.09.205> PMID: 30253367
90. Fleckenstein JH, Niswonger RG, Fogg GE. River-aquifer interactions, geologic heterogeneity, and low-flow management. *Ground Water*. 2006; 44(6):837–52. <https://doi.org/10.1111/j.1745-6584.2006.00190.x> PMID: 17087756
91. Gailey RM, Fogg GE, Lund JR, Medellín-Azuara J. Maximizing on-farm groundwater recharge with surface reservoir releases: a planning approach and case study in California, USA. *Hydrogeology Journal*. 2019; 27(4):1183–206. <https://doi.org/10.1007/s10040-019-01936-x>
92. Feurdean A, Ruprecht E, Molnár Z, Hutchinson SM, Hickler T. Biodiversity-rich European grasslands: Ancient, forgotten ecosystems. *Biological Conservation*. 2018; 228(May):224–32. <https://doi.org/10.1016/j.biocon.2018.09.022>
93. Eaton MR. Restoration of natural flooding process on the Cosumnes River Preserve. Overview and status report. San Francisco, CA: The Nature Conservancy, 1998.
94. Huff TM, DiGaudio R. Songbird monitoring on the Cosumnes River Preserve: progress report of the 1999 field season. Stinson Beach, CA: Point Reyes Bird Observatory Report to The Nature Conservancy, 2000.
95. Tu IYM. Vegetation patterns and processes of natural regeneration in periodically flooded riparian forests in the Central Valley of California 2000.
96. Trowbridge WB. The role of stochasticity and priority effects in floodplain restoration. *Ecological Applications*. 2007; 17(5):1312–24. <https://doi.org/10.1890/06-1242.1> PMID: 17708210
97. Hutchinson R, Fremier A, Viers J. Interaction of restored hydrological connectivity and herbicide suppresses dominance of a floodplain invasive species. *Restoration Ecology*. 2020;1–10. <https://doi.org/10.1111/rec.13240>
98. Ribeiro F, Crain PK, Moyle PB. Variation in condition factor and growth in young-of-year fishes in floodplain and riverine habitats of the Cosumnes River, California. *Hydrobiologia*. 2004; 527(1):77–84. <https://doi.org/10.1023/B:HYDR.0000043183.86189.f8>
99. Sheibley RW, Ahearn DS, Dahlgren RA. Nitrate loss from a restored floodplain in the Lower Cosumnes River, California. *Hydrobiologia*. 2006; 571(1):261–72. <https://doi.org/10.1007/s10750-006-0249-2>
100. Hoagland BW, Schmidt C, Russo TA, Adams R, Kaye J. Controls on nitrogen transformation rates on restored floodplains along the Cosumnes River, California. *Science of the Total Environment*. 2019; 649:979–94. <https://doi.org/10.1016/j.scitotenv.2018.08.379> PMID: 30179826

101. Beagle JR, Whipple AA, Grossinger RM. Landscape Patterns and Processes of the McCormack-Williamson Tract and Surrounding Area: A framework for restoring a resilient and functional landscape. Richmond, CA: 2013.
102. D'Elia AH, Liles GC, Viers JH, Smart DR. Deep carbon storage potential of buried floodplain soils. *Scientific Reports*. 2017; 7(1):1–7. <https://doi.org/10.1038/s41598-017-06494-4> PMID: 28811477
103. Hammersmark CT, Fleenor WE, Schladow SG. Simulation of a flood impact and habitat extent for a tidal freshwater marsh restoration. *Ecological Engineering*. 2005; 25:137–52. <https://doi.org/10.1016/j.ecoleng.2005.02.008>
104. Florsheim JL, Mount JF, Hammersmark C, Fleenor WE, Schladow GS. Geomorphic Influence on Flood Hazards in a Lowland Fluvial-Tidal Transitional Area, Central Valley, California. *Natural Hazards Review*. 2008; 9(3):116–24. [https://doi.org/10.1061/\(asce\)1527-6988\(2008\)9:3\(116\)](https://doi.org/10.1061/(asce)1527-6988(2008)9:3(116))
105. Dietterick BC, White R, Hilburn R. Comparing LiDAR-Generated to Ground- Surveyed Channel Cross-Sectional Profiles in a Forested Mountain Stream. *Coast redwood forests in a changing California: A symposium for scientists and managers*. 2012:639–48.
106. Wheaton JM, Brasington J, Darby SE, Sear DA. Accounting for uncertainty in DEMs from repeat topographic surveys: Improved sediment budgets. *Earth Surface Processes and Landforms*. 2010; 35(2):136–56. <https://doi.org/10.1002/esp.1886>
107. Partners O. 2007 California Department of Water Resources Topographic LiDAR: San Joaquin Delta. NOAA National Celeters for Environmentla Information: <https://www.fisheries.noaa.gov/inport/item/>; 2007.
108. Constantine CR, Mount JF, Florsheim JL. The effects of longitudinal differences in gravel mobility on the downstream fining pattern in the Cosumnes River, California. *Journal of Geology*. 2003; 111(2):233–41. <https://doi.org/10.1086/345844>
109. Kondolf GM. Hungry water: Effects of dams and gravel mining on river channels. *Environmental Management*. 1997; 21(4):533–51. <https://doi.org/10.1007/s002679900048> PMID: 9175542
110. Abbe TB, Montgomery DR. Large woody debris jams, hydraulics and habitat formation in large rivers. *Regulated Rivers: Research & Management*. 1996; 12:201–21. [https://doi.org/10.1002/\(sici\)1099-1646\(199603\)12:2](https://doi.org/10.1002/(sici)1099-1646(199603)12:2).
111. Wohl E, Scott DN. Wood and sediment storage and dynamics in river corridors. *Earth Surface Processes and Landforms*. 2017; 42(1):5–23. <https://doi.org/10.1002/esp.3909>
112. Pawley A, Moldoff D, Brown J, Freed S. Reducing flood risk and improving system resiliency in Sacramento, California: overcoming obstacles and emerging solutions. *Frontiers in Water*. 2023; 5:1188321. <https://doi.org/10.3389/fw.2023.1188321>
113. Mississippi River Flood History 1543–Present. New Orleans/Baton Rouge Weather Forcast Office: National Weather Service, 2019.
114. Lehmkühl F, Schüttrumpf H, Schwarzbauer J, Brüll C, Dietze M, Letmathe P, et al. Assessment of the 2021 summer flood in Central Europe. *Environmental Sciences Europe*. 2022; 34(1). <https://doi.org/10.1186/s12302-022-00685-1>
115. Record rainfall brings floods and swollen rivers. Dutch Water Sector, 2021.
116. Ludwig P, Ehmele F, Franca MJ, Mohr S, Caldas-Alvarez A, Daniell JE, et al. A multi-disciplinary analysis of the exceptional flood event of July 2021 in central Europe. Part 2: Historical context and relation to climate change. 2022.
117. Verweij S, Busscher T, van den Brink M. Effective policy instrument mixes for implementing integrated flood risk management: An analysis of the 'Room for the River' program. *Environmental Science & Policy*. 2021; 116:204–12. <https://doi.org/10.1016/j.envsci.2020.12.003>
118. Thaler T, Hudson P, Viavattene C, Green C. Natural flood management: Opportunities to implement nature-based solutions on privately owned land. *WIREs Water*. 2023; 10(3). <https://doi.org/10.1002/wat2.1637>
119. Ungvári G, Kis A. Reducing flood risk by effective use of flood-peak polders: A case study of the Tisza River. *Journal of Flood Risk Management*. 2022; 15(3). <https://doi.org/10.1111/jfr3.12823>
120. Turkelboom F, Demeyer R, Vranken L, De Becker P, Raymaekers F, De Smet L. How does a nature-based solution for flood control compare to a technical solution? Case study evidence from Belgium. *Ambio*. 2021. <https://doi.org/10.1007/s13280-021-01548-4> PMID: 33974215
121. Gell PA, Reid MA, Wilby RL. Management pathways for the floodplain wetlands of the southern Murray–Darling Basin: Lessons from history. *River Research and Applications*. 2019. <https://doi.org/10.1002/rra.3515>